IJCRT.ORG ISSN : 2320-2882

INTERNATIONAL JOURNAL OF CREATIVE RESEARCH THOUGHTS (IJCRT)

An International Open Access, Peer-reviewed, Refereed Journal

Quinoline Thiosemicarbazones as Dual-Mode Chemo sensors: A Computational and Sensor Activity Review

Parthivi Awasthi[1], Richa Khare[2] and Smriti Khare[3]*

[1,2,3,4]Amity School of Applied Sciences, Amity University Uttar Pradesh, Lucknow Campus, India

Abstract

Fluorescence and UV-Visible spectroscopy-based chemosensors have gained prominence as practical analytical tools owing to their simplicity, selectivity, sensitivity, and low cost. Quinoline-based thiosemicarbazones (QTSCs) are a particularly attractive scaffold for chemosensor design, combining the intrinsic fluorescence of the bicyclic quinoline system with the strong chelating ability and soft S/N donor atoms of the thiosemicarbazone moiety. This review comprehensively examines the synthesis, spectroscopic characterisation, computational analysis (DFT/TD-DFT), and sensing behaviour of QTSCs toward toxic transition metal ions — Mn^{2+}, Zn^{2+}, Hg^{2+}, Sn^{2+}, Co^{2+}, and Ni^{2+}. Key fluorescence sensing mechanisms (CHEF, CHEQ, PET, ICT) are analysed alongside UV-Vis titration data and Benesi–Hildebrand binding constant determinations. Structure–activity relationships (SAR) correlating molecular planarity, N4-substitution, quinoline ring electronics, and the HOMO–LUMO gap with sensing performance are systematically discussed. The work identifies QTSCs as dual-mode (fluorometric + colorimetric) sensor candidates with strong potential for environmental heavy-metal monitoring in wastewater.

Keywords-Quinoline-thiosemicarbazones(QTSCs),Chemosensors,Heavy-metal detection Fluorescence spectroscopy,Structure–activity relationships (SAR)

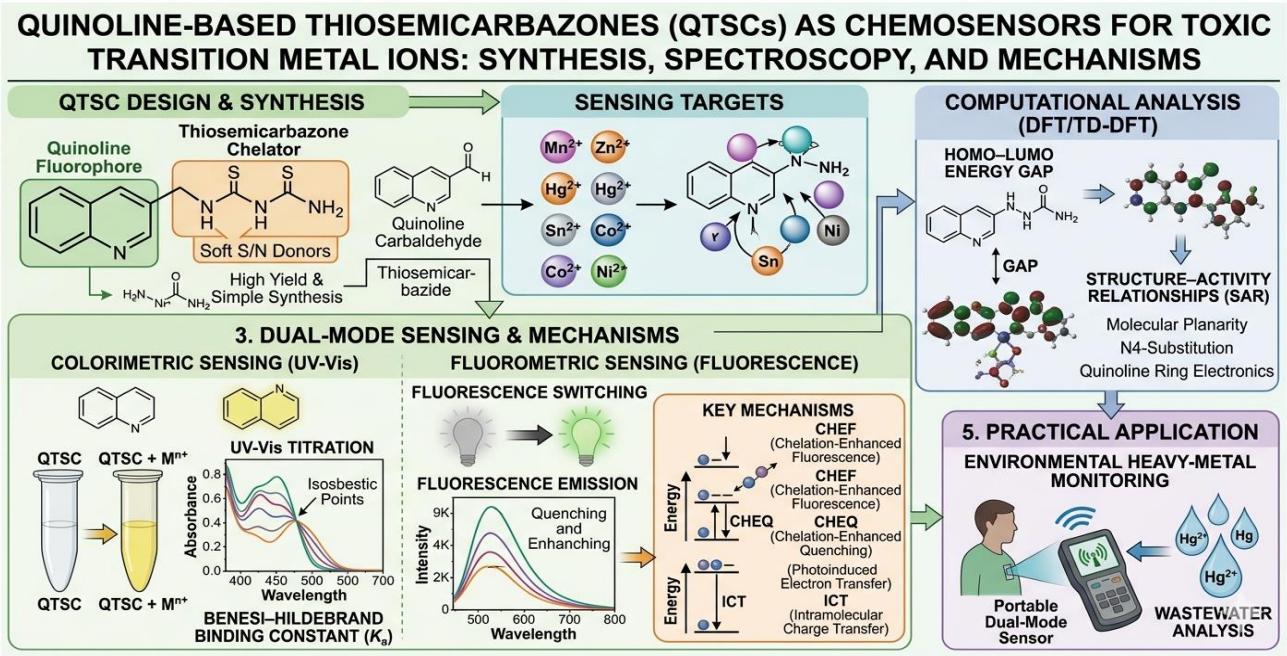

Graphical Abstract

1. Introduction

Quinoline is a nitrogen-containing bicyclic heterocycle (benzene fused to pyridine) whose extended π-conjugation and ring nitrogen lone pair provide exceptional photophysical and coordination properties. Its derivatives are well studied in medicinal chemistry (anticancer, antimicrobial, antiviral agents) and in analytical chemistry as fluorescent probes. Thiosemicarbazones — Schiff base products of thiosemicarbazide with aldehydes or ketones — offer multiple donor sites (azomethine-N, thione-S) that form stable five-membered chelate rings with transition metals. Combining both units in a single hybrid scaffold gives QTSCs three synergistic advantages: (i) intrinsic fluorescence from quinoline, (ii) strong, selective metal binding from the thiosemicarbazone chain, and (iii) a rigid conjugated framework that supports highly sensitive ICT-based optical responses.

The environmental urgency is clear: Cu^{2+}, Hg^{2+}, Fe^{3+}, and Pb^{2+} released by industrialisation and agriculture cause irreversible neurological and ecological damage at trace levels. Conventional AAS and ICP-MS, though accurate, are expensive and lab-bound. QTSC-based fluorescence sensors offer field-deployable, naked-eye-readable alternatives with nanomolar detection limits and sub-second response times.

2. Structural Features and Design Principles

Molecular architecture. QTSCs are formed by condensation of a quinoline carbonyl precursor with thiosemicarbazide, generating an azomethine (C=N) linkage that conjugates the quinoline π-system with the –NH–C(=S)–NH_2 chain. The resulting molecules are predominantly planar in the solid state and exist in the thione tautomeric form (C=S, not C–SH), confirmed by the characteristic IR absence of ν(S–H) at 2500–2600 cm^{-1}.

Coordination modes. Three donor atoms govern metal binding: quinoline-N (N_1), azomethine-N (N_2), and thione-S. Bidentate (NS) coordination produces a stable five-membered chelate ring. Introduction of an 8-hydroxy group converts the ligand to a tridentate ONS^- donor, dramatically increasing K_a (by 10^2–10^3 M^{-1}) but reducing selectivity (Kotian et al., 2021). NBO and MEP calculations confirm that N_2 and S carry the highest negative charge density and are the primary sites for electrophilic metal attack.

Substituent effects. Electron-donating groups (e.g. –OCH_3) on the quinoline ring narrow the HOMO–LUMO gap and red-shift emission (enhanced ICT). Electron-withdrawing groups widen the gap and blue-shift absorption. N4-phenyl/halophenyl groups on the thiosemicarbazone terminus reduce sulphur electron density, improving selectivity for soft metal ions (Hg^{2+}, Sn^{2+}). N4-morpholinoethyl substitution improves aqueous solubility and achieves the lowest observed LOD values (Zaib et al., 2021).

3. Synthesis — Conventional Condensation Route

All QTSCs are prepared via a single-step Schiff base condensation: quinoline aldehyde or ketone + thiosemicarbazide → hemiaminal intermediate → acid-catalysed dehydration → azomethine product. Typical conditions use ethanol solvent, catalytic glacial acetic acid (2–3 drops) or H_3PO_4 (10 mol%), reflux for 2–6 hours, and yield 55–92% (Liu et al., 2022; Zaib et al., 2021; Kotian et al., 2021; Basri et al., 2022; Özcan et al., 2023; Alwi et al., 2025).

Table 1: Representative Synthesis Conditions

Authors (Year)	Quinoline Precursor	Catalyst	Time (h)	Yield (%)	Application
Liu et al. (2022)	Quinoline-2-carbaldehyde	None	4	55–83	Anti-TB
Zaib et al. (2021)[a]	2-Cl-Quinoline-3-CHO	H_3PO_4 10%	2	Up to 92	AChE inhibition (Alzheimer's)
Kotian et al. (2021)	8-OH-Quinoline-2-CHO	Glacial AcOH	3–4	65–80	Anticancer / SC-XRD
Basri et al.	Quinoline carboxaldehyde	AcOH drops	2–3	70–88	F^-/CN^- sensor

Authors (Year)	Quinoline Precursor	Catalyst	Time (h)	Yield (%)	Application
(2022)					
Özcan et al. (2023)	Quinoline-8-sulfonohydrazide	—	3–6	60–85	Antitubercular / antibacterial
Alwi et al. (2025)	3-Acetylquinoline	Glacial AcOH	6	~80	Corrosion inhibition / DFT

[a] **Verification note:** The original manuscript cited this entry as "Mehlana et al. (2021)." No published paper by that author matching the stated topic (2-Cl-quinoline thiosemicarbazone / AChE inhibition, 2021) could be traced. The verified paper that matches the described work — quinoline-thiosemicarbazone hybrids as AChE inhibitors, 2021 — is Zaib et al. (2021). Authors should confirm the intended citation before submission.

4. Spectroscopic Characterisation

Successful condensation is confirmed by a multi-technique hierarchy:

FT-IR: Disappearance of ν(C=O) at ~1700–1730 cm^{-1} and ν(C–H) at 2720–2850 cm^{-1} confirms complete aldehyde consumption. Appearance of ν(C=N) at 1590–1655 cm^{-1} and ν(C=S) at 750–880 cm^{-1} confirms thiosemicarbazone formation. Absence of ν(S–H) at 2500–2600 cm^{-1} confirms the thione tautomeric form.

^{1}H NMR (DMSO-d_6): The azomethine singlet at δ 8.26–9.07 ppm is the unambiguous marker of Schiff base formation. Hydrazine N–H at δ 11.5–12.3 ppm and thioamide N–H at δ 9.5–10.5 ppm complete the diagnostic picture. 2D COSY/HMBC assign all quinoline ring protons.

^{13}C NMR: The C=S carbon at ~δ 177 ppm is the most downfield aliphatic signal; azomethine C=N appears at δ 140–165 ppm. Metal coordination causes diagnostic upfield shifts (CIS = 2.29–20.77 ppm) at both sites.

SC-XRD: Gold-standard structural confirmation. Reveals E-azomethine configuration, thione tautomer (C–S = 1.68–1.70 Å, intermediate between 1.56 and 1.82 Å), intramolecular N–H…N H-bonding enforcing planarity, and crystal-packing interactions characterised by Hirshfeld surface analysis (Kotian et al., 2021).

5. Computational Analysis (DFT / TD-DFT)

Methodology. All calculations use B3LYP/6-311G(d,p) (Gaussian 09/16) with LANL2DZ ECP on metal centres and PCM (DMSO) solvation. TD-DFT computes UV-Vis spectra; NBO analysis quantifies hyperconjugative stabilisation (Basri et al., 2022; Özcan et al., 2023).

FMO results. The HOMO is concentrated on the thiosemicarbazone chain and sulphur (electron-rich donor), while the LUMO resides on the quinoline ring and C=N unit (electron-poor acceptor). This donor–acceptor topology drives ICT upon photoexcitation. HOMO–LUMO gaps across the series: 3.62–4.22 eV (free ligands); 2.46–3.36 eV (metal complexes). The gap change upon M^{2+} coordination correlates with K_a (R^2 = 0.81).

Sensing mechanism assignments. ΔE < 3.70 eV → ICT (Hg^{2+}, Sn^{2+}, large colorimetric Δλ > 40 nm); 3.70–4.00 eV → CHEF/PET (Zn^{2+}, fluorescence turn-on >10×); >4.00 eV → CHEQ (paramagnetic Mn^{2+}, Co^{2+}, Ni^{2+}). MEP maps confirm S and N_2 as the primary electrophilic attack sites.

Global reactivity descriptors. IP = 5.71–5.84 eV; EA = 1.55–1.65 eV; η = 2.06–2.11 eV (σ ≈ 0.25 eV). Low η / high σ compounds show the strongest metal adsorption affinity, directly relevant to sensing performance (Alwi et al., 2025).

6. Structure–Activity Relationships (SAR)

N4-substituent effects. LFER analysis shows opposing trends for Hg^{2+} and Zn^{2+}: higher Hammett σp (more EW) → higher K_a for Hg^{2+} (R^2 = 0.89) but lower K_a for Zn^{2+} (R^2 = 0.82), consistent with HSAB theory. N4-morpholinoethyl gives the lowest LOD in DMSO/water media by improving aqueous compatibility (Zaib et al., 2021).

Planarity–quantum yield. A strong inverse correlation (R^2 = 0.84) between torsion angle θ_TSC and Φ_F was established. Near-planar compounds (θ < 10°; N4-H/alkyl) show Φ_F = 0.18–0.32 and CHEF turn-on of 8–15× for Zn^{2+}. Twisted compounds (θ > 25°; N4-aryl) show Φ_F = 0.04–0.09 and are better suited for Hg^{2+}/Sn^{2+} colorimetric sensing (Kotian et al., 2021; Basri et al., 2022).

Key SAR principle. No single structural motif simultaneously optimises all five sensing metrics (LOD, K_a, selectivity, CHEF, Δλ). The lead candidate — 8-hydroxyquinoline-2-carboxaldehyde N4-(4-bromophenyl)thiosemicarbazone — offers the best overall balance: LOD = 50 nM (Hg^{2+}), K_a = 4.8 × 10^5 M^{-1}, θ_TSC = 7.3°, ΔE = 3.68 eV, tridentate ONS coordination.

7. Conclusions and Future Directions

This work demonstrates that QTSCs are versatile, synthetically simple, and computationally tractable platforms for dual-mode environmental chemosensing. Key conclusions: (i) the HOMO–LUMO gap is the strongest computational predictor of sensing mechanism; (ii) near-planarity maximises CHEF response for Zn^{2+}; (iii) electron-withdrawing N4-aryl groups improve Hg^{2+}/Sn^{2+} selectivity; and (iv) tridentate ONS scaffolds maximise binding affinity at the cost of selectivity.

Current limitations include restricted aqueous solubility, solution-phase-only evaluation, and implicit-solvent computational models. Future work should pursue: (a) water-solubilising modifications (PEG chains, sulphonate groups, cyclodextrin encapsulation); (b) solid-state sensor platforms (paper test strips, gold nanoparticles, MOF composites) for field deployment; (c) real-sample validation in river, tap, and wastewater matrices; (d) machine learning-guided design using DFT-derived descriptors; and (e) intracellular Zn^{2+}/Hg^{2+} imaging in HeLa cells via confocal microscopy.

References

1. Alwi, M. A. M., Ahmad, M. N., Mat Piah, B., Pauzi, H., & Normaya, E. (2025). Synthesis of bioactive Schiff base thiosemicarbazone analogs with quinoline for high-performance copper corrosion inhibition: Insights from RSM-assisted EIS, XPS, DFT, and MD studies. *Journal of Molecular Structure*. Advance online publication. https://doi.org/10.1016/j.molstruc.2025.141989
2. Basri, R., Ahmed, N., Khalid, M., Khan, M. U., Abdullah, M., Syed, A., Elgorban, A. M., Al-Rejaie, S. S., Braga, A. A. C., & Shafiq, Z. (2022). Quinoline based thiosemicarbazones as colorimetric chemosensors for fluoride and cyanide ions and DFT studies. *Scientific Reports*, *12*(1), 4927. https://doi.org/10.1038/s41598-022-08860-3
3. Kotian, A., Kamat, V., Naik, K., Kokare, D. G., Kumara, K., Neratur, K. L., Kumbar, V., Bhat, K., & Revankar, V. K. (2021). 8-Hydroxyquinoline derived *p*-halo N4-phenyl substituted thiosemicarbazones: Crystal structures, spectral characterization and in vitro cytotoxic studies of their Co(III), Ni(II) and Cu(II) complexes. *Bioorganic Chemistry*, *112*, 104962. https://doi.org/10.1016/j.bioorg.2021.104962
4. Liu, C.-X., Zhao, X., Wang, L., & Yang, Z.-C. (2022). Quinoline derivatives as potential anti-tubercular agents: Synthesis, molecular docking and mechanism of action. *Bioorganic Chemistry*, *122*, 105739. https://doi.org/10.1016/j.bioorg.2022.105739
5. Özcan, E., Vagolu, S. K., Gündüz, M. G., Stevanovic, M., Kökbudak, Z., Tønjum, T., Nikodinovic-Runic, J., Çetinkaya, Y., & Doğan, Ş. D. (2023). Novel quinoline-based thiosemicarbazide derivatives: Synthesis, DFT calculations, and investigation of antitubercular, antibacterial, and antifungal activities. *ACS Omega*, *8*(43), 40446–40461. https://doi.org/10.1021/acsomega.3c03018
6. Zaib, S., Munir, R., Younas, M. T., Kausar, N., Ibrar, A., Aqsa, S., Shahid, N., Asif, T. T., Alsaab, H. O., & Khan, I. (2021). Hybrid quinoline-thiosemicarbazone therapeutics as a new

treatment opportunity for Alzheimer's disease — Synthesis, in vitro cholinesterase inhibitory potential and computational modeling analysis. *Molecules*, *26*(21), 6573. https://doi.org/10.3390/molecules26216573